

SiO₂/Si interfacial structure on vicinal Si(100) studied with second-harmonic generation

G. Lüpke, D. J. Bottomley, and H. M. van Driel

Department of Physics, University of Toronto, Toronto, Ontario, Canada M5S 1A7

(Received 2 December 1992)

Surface second-harmonic generation (SHG) has been used to reveal the symmetry characteristics of buried interfaces on oxidized vicinal Si(100). For native oxides, onefold and threefold symmetries are prominent, arising from the presence of steps and ordered Si-O bonds in the vicinity of the steps, respectively. For thermal oxides grown at 900 °C, twofold symmetry is most prominent, consistent with the presence of highly oriented microcrystallites at the buried interface. SHG measurements of postoxidation annealing of oxides grown in steam are consistent with the amount of stress reduction occurring as a result of annealing being too small to be observed by SHG, and with hydrogen leaving the buried interface below 600 °C.

I. INTRODUCTION

The SiO₂/Si(100) interface has been the subject of intense study due to its important role in semiconductor technology. One fundamental issue concerns the atomic mechanisms by which the structural and chemical transitions from Si(100) to amorphous SiO₂ occur in the interfacial region. Several experimental techniques have been used in an attempt to determine the structure of the interface, its extent, and its roughness.¹⁻¹⁹ Previous studies generally agree in identifying two distinct regions. The region near the interface consists of a few atomic layers containing Si atoms in intermediate oxidation states.¹⁻⁴ A second region extends about 30 Å into the SiO₂ overlayer.¹ The SiO₂ in this layer is compressed because the number density of Si atoms in Si is higher than in SiO₂.¹ Several structural models have been proposed for the transition from Si(100) to amorphous SiO₂, each predicting a characteristic distribution of oxidation states.^{1,5}

There have been theoretical predictions of a boundary layer of microcrystallites between the Si substrate and the amorphous overlayer which allows the long-range order to decay gradually into the amorphous film.²⁰ Clear evidence for the presence of crystalline order in the interfacial SiO₂ layer was seen in the work of Fuoss *et al.*⁶ In that work, x-ray-diffraction peaks from small crystallites were found. Similar experiments performed by Rochet *et al.* clearly show the presence of microcrystallites at the interface of a misoriented Si(100) substrate.⁷ Photoemission studies performed by Niwano *et al.* are also consistent with crystalline order being present in the interfacial region.² All three of these papers put the existence of SiO₂ microcrystallites in oxide layers grown at relatively high temperatures ($T \gtrsim 700$ °C) on a firm footing. However, the conclusions drawn from data for oxides grown at lower temperatures are more controversial. High-resolution transmission electron microscopy (TEM) measurements of Ourmazd *et al.* appear to indicate the existence of a transition interfacial layer between the SiO₂ film and the Si(100) substrate which could possibly be tridymite, a high-temperature polymorph of crystalline

SiO₂.^{3,5,8} But modeling by Akatsu and Ohdomari⁹ of TEM images from amorphous oxide layers with no intervening *c*-SiO₂ yielded images consistent with those observed by Ourmazd *et al.* Core-level spectroscopy (CLS) work performed by Himpfel *et al.* showed a substantial concentration of Si atoms in intermediate oxidation states, implying that the interface is not perfectly abrupt on an atomic scale, and that either the interface is extended over a few layers, or that it is disordered.¹ However, by using grazing-incidence x-ray scattering Renaud *et al.* later obtained evidence of an epitaxial interfacial layer which contained a significant amount of both order and disorder on an atomic scale.¹⁰ Nevertheless, the presence and structure of the epitaxial oxide have remained highly controversial, mainly because of the inability of electron diffraction to yield diffraction peaks which can be assigned unambiguously.

In this paper we use optical second-harmonic generation (SHG) to determine the macroscopic symmetry properties of the interfacial SiO₂ layer and to investigate the possibility of crystalline order present at the SiO₂/Si interface on vicinal Si(100) surfaces, prepared under various conditions. The surface SHG technique has been reviewed by Shen²¹ and Richmond *et al.*²² In general, optical methods can probe the interface of two condensed media if one of them is transparent to the probing optical beam. This fact gives an important advantage to optical methods over other techniques which are based on particle beam scattering and diffraction. However, the linear-optical response of the interface usually provides little information on possible *crystalline* structures of the interfacial layer between the two media since the linear-optical parameters are scalar in cubic media. In contrast, the symmetry characteristics resolved by the higher-order nonlinear optical susceptibilities are indicative of the symmetry of the interfacial structure. Thus the optical second-harmonic (SH) response turns out to be sensitive to any modification of the interfacial layer structure as has been clearly shown in a number of experiments in recent years.^{11,12,23,24}

The outline of this paper is as follows. In Sec. II we discuss the phenomenology of the symmetry properties of

the SH intensity dependence on sample azimuthal angle for vicinal Si(100) surfaces, as well as the possible microscopic origins of the SH intensity. In Sec. III we define our experimental conditions and present data obtained from oxides prepared under various conditions. In Sec. IV we discuss the implications of the data obtained from the various oxides on the interfacial structure including the influence of mechanical stress, step-induced defects, bonded hydrogen, and crystalline order present at the interface. Section V contains our conclusions.

II. THEORY

In the experiments reported below, we concentrate on the p -polarized SH response $I_{s,p}^{(2\omega)}$ for an s -polarized fundamental field $E^{(\omega)}$ since this polarization combination contains one isotropic and most of the anisotropic nonlinear susceptibility tensor elements.²⁵ The theoretical dependence of the SH intensity on the sample azimuthal angle ψ from the flat Si(100) surface is well known: the surface yields only an isotropic response, and therefore SHG is insensitive to surface symmetry. The electric dipole-allowed interfacial contribution originates from broken inversion symmetry normal to the interface and is isotropic with respect to variation of ψ . The bulk nonlinear polarization density in Si(100) is magnetic dipole or electric quadrupole in character and gives rise to an anisotropic contribution with C_{4v} symmetry in addition to an isotropic contribution. For vicinal Si(100), interfacial anisotropic contributions to SHG up to threefold in symmetry are permitted, enabling the structural symmetry present to be deduced. This approach is not limited to Si(100), but applies quite generally to all the (100) surfaces of cubic centrosymmetric media. The dependence of $I_{s,p}^{(2\omega)}$ on ψ is given phenomenologically by a truncated Fourier expansion²⁵

$$I_{s,p}^{(2\omega)}(\psi) \propto |\chi_t^{(2)}|^2 (I_s^{(\omega)})^2 = \left| \sum_{m=0}^4 c_m \cos(m\psi) \right|^2 (I_s^{(\omega)})^2, \quad (1)$$

where $\chi_t^{(2)}$ is the total second-order susceptibility, the c_m are linear combinations of $\chi_t^{(2)}$ tensor elements, which are, in general, complex quantities, and $I_s^{(\omega)}$ is the s -polarized fundamental beam intensity. We note that, in general, $\chi_t^{(2)}$ contains contributions from the Si(100) surface-dipole and bulk-quadrupole sources,²⁵ as well as contributions that are caused by stress,¹¹ static electric fields, or noncentrosymmetric crystalline phases of SiO₂ at the interface.¹²

Using Eq. (1) to fit the experimental data reported below we have deduced the relative values of the c_m for various SiO₂/Si(100) interfaces. Because of the large isotropic c_0 coefficient it is impossible to determine small relative phases between the anisotropic c_m and c_0 under the s -input and p -output polarization combination alone. However, these can be determined by measuring the s -polarized SH output, when the analyzer is slightly rotated away from s polarization, in order to introduce a small amount of the isotropic term.²⁶ Including these measurements in our analysis we found the relative phase of the complex c_m with respect to c_0 to be 0° or 180° with an accuracy of $\pm 10^\circ$ indicating that to a good approximation

the c_m are real and that spectroscopically we are in a nonresonant regime for the oxidized surface. Note that because interfacial SHG is described by a third rank tensor, all interfacial symmetries higher than C_{3v} yield an isotropic response; c_4 arises only from bulk sources and is independent of *any* interfacial modification.²⁵ In contrast to SHG from vicinal Si(111) surfaces where c_3 has both bulk and interfacial contributions,^{23,24} and will vary with surface preparation, we can normalize the c_m to c_4 for vicinal Si(100) surfaces.²⁷

III. EXPERIMENTAL CONDITIONS AND RESULTS

For SHG we used a mode-locked Ti:sapphire laser operating at a wavelength of 765 nm (1.63 eV), generating a train of 130-fs pulses at 76 MHz with an average power of 0.8 W. In all experiments the beam was focused on the sample to a 40- μ m-diam spot at an angle of incidence of 45°. The SH intensity was measured with a photomultiplier tube and a gated photon counter as a function of ψ , which we define as the angle between the plane of incidence and the [011] axis.

To investigate the symmetry characteristics of the buried interface, we have measured the SH response from the SiO₂/Si(100) interface on vicinal Si(100) after oxide growth in various environments. Oxides were grown in steam at 550°C, and in dry O₂ at 100 and 900°C. Samples with three different vicinal angles α were studied: $\alpha=0^\circ$, 2° , and 5° (all $\pm \frac{1}{2}^\circ$). The miscut direction was towards [011], producing a regular step structure with different step densities.²⁸ The wafers were n type ($\sim 60 \Omega \text{ cm}$; P doped) with a native oxide grown in steam at 550°C and are referred to henceforth as the native oxide in steam (NOS) samples. This preparation temperature is expected to result in monatomic steps at the interface.²⁸

To determine the influence of the oxide layer on the

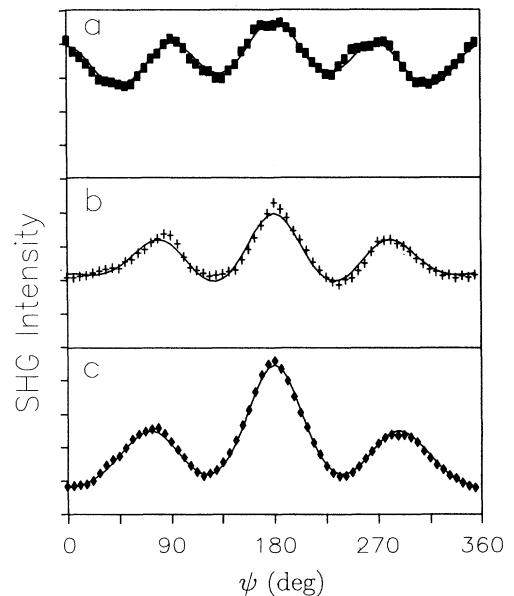


FIG. 1. $I_{s,p}^{(2\omega)}(\psi)$ from the NOS samples with vicinal angles α of (a) 0° ; (b) 2° ; (c) 5° .

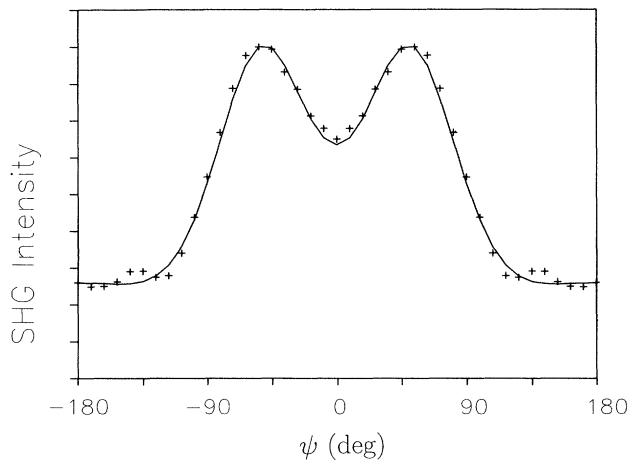


FIG. 2. $I_{s,p}^{(2\omega)}(\psi)$ from the $\alpha=5^\circ$ clean surface.

symmetry characteristics of the vicinal surface as observed by SHG, we have measured $I_{s,p}^{(2\omega)}(\psi)$ from the $\alpha=5^\circ$ surface in an ultrahigh vacuum (UHV) chamber with a base pressure below 6×10^{-10} Torr. An almost single domain low-energy electron diffraction pattern was obtained from the sample after heating it to 1200 °C and cooling from 900 °C at $\sim 1^\circ \text{C s}^{-1}$ to room temperature. The surface contamination was found to be below the Auger electron spectroscopy $\approx 1\%$ limit. The sample was mounted on a holder which permitted azimuthal rotation of 180° while in UHV.

We consider first the SHG results from the NOS samples. Figure 1 shows $I_{s,p}^{(2\omega)}(\psi)$ from the NOS samples in air for different α . The response for $\alpha=0^\circ$, indicated in Fig. 1(a), is well known and is dominated by isotropic and C_{4v} symmetry contributions.²⁵ However, for $\alpha \neq 0^\circ$ the C_{4v} symmetry is clearly broken as indicated in Figs. 1(b) and 1(c). Deviation from C_{4v} symmetry clearly increases with increasing α . In Fig. 1 all three curves are symmetric about $\psi=0^\circ, 180^\circ$, confirming that the step structure preserves the (01 $\bar{1}$) mirror plane. For the vicinal NOS surfaces, two anisotropic coefficients emerge and dominate: c_1 and c_3 . We observe that c_1 and c_3 are (approximately) linear functions of α , consistent with a step-induced contribution whose magnitude necessarily scales with $\tan \alpha$. Table I lists the values of the c_m coefficients deduced from the data in Fig. 1(c).

To prove that the SiO₂ at the interface has a substantial influence on the SHG process, we have measured $I_{s,p}^{(2\omega)}(\psi)$ for the clean $\alpha=5^\circ$ surface in UHV. Figure 2 shows $I_{s,p}^{(2\omega)}(\psi)$ thus obtained; the c_m coefficients are listed

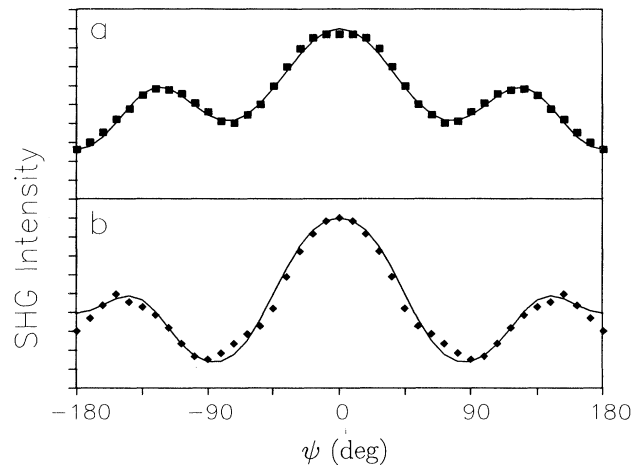


FIG. 3. $I_{s,p}^{(2\omega)}(\psi)$ from the $\alpha=5^\circ$ surface thermally oxidized at (a) 100 °C; (b) 900 °C.

in Table I. Because of the mirror symmetry present in Fig. 1 about $\psi=0^\circ, 180^\circ$ we have mirror-imaged the data at $\psi=0^\circ$ to show a complete rotation. The symmetry characteristics revealed by Figs. 1(c) and 2 are very different, indicating that SHG is extremely sensitive to the interfacial structure. The most striking difference is the increase in c_2 for the clean surface. The occurrence of a significant c_2 shows the predominance of the (1 \times 2) Si-Si dimer structure on the clean sample due to biatomic steps, yielding a terrace distribution with net C_{2v} symmetry.²⁸ Sensitivity of SHG to the dimers is expected since the fundamental photon energy is near the dimer surface state energy.¹³ In qualitative agreement with Hollering, Dijkkamp, and Elswijk,²³ c_0 changes by a factor of -3 when the oxide is removed. There is still a net $c_3 \sim -\frac{1}{3}c_1$, which is not surprising because there are two possible contributions to c_3 : the bulk contribution due to the misorientation²⁷ and a trigonometric effect arising from C_{1v} step symmetry.²⁹

To investigate further the effect of oxide growth conditions on the structure of the SiO₂/Si interface we have oxidized the clean $\alpha=5^\circ$ surface at different temperatures. A low-temperature oxidation (LTO) at 100 °C and a high-temperature oxidation (HTO) at 900 °C were performed with an exposure to 3000 L of dry O₂ (1 L = 10^{-6} Torr s) at a pressure of 2×10^{-5} Torr. The steps on the clean surface prior to LTO were mainly biatomic, whereas for HTO they were monatomic.²⁸ Figures 3(a) and 3(b) show $I_{s,p}^{(2\omega)}(\psi)$ for LTO and HTO, respectively,

TABLE I. Fourier coefficients from Si(100):5° deduced from the SHG data normalized using $c_4=1$.

Treatment	Fig. no.	c_0	c_1	c_2	c_3	Remarks
NOS, 550 °C	1(c)	13	-2.4	0.3	-3.2	monatomic steps
clean, 100 °C	2	-36	-11	1.9	4.1	biatomic steps
LTO, 100 °C	3(a)	-28	-4.3	-1.4	-3.7	biatomic steps
HTO, 900 °C	3(b)	-16	-2.3	-4.6	-1.8	monatomic steps
H covered, 100 °C		14	-1.9	-1.1	-3.2	biatomic steps, dihydride

mirror imaged at $\psi=0^\circ$; the c_m coefficients are listed in Table I.

IV. DISCUSSION

A. Native oxide samples

First we discuss the SH rotational anisotropy of the NOS and LTO samples. We observe that c_0 is independent of α , which is in agreement with the invariance of the CLS results of Himpel *et al.* with vicinal angle, suggesting that the SiO_2 sublayer is not affected significantly by the presence of steps.¹ In general, the c_1 coefficient arises from the stepped surface and is indicative of its C_{1v} symmetry.^{23,24} However, for the NOS sample, $|c_3|$ actually exceeds $|c_1|$ and therefore is strongly suggestive of the presence of ordered Si-O bonds in the vicinity of the steps.

We note that c_3 is a linear function of $\tan\alpha$ for $\alpha \leq 5^\circ$ which implies that c_3 is not generated over the entire terrace. To estimate the in-plane extension of the hypothetical SiO_2 sublayer with C_{3v} symmetry, we have compared the absolute magnitude of c_3 in Fig. 1(c) with the d_{11} susceptibility tensor element of α -quartz which arises from its D_3 symmetry.³⁰ This approach is reasonable because in both cases the nonlinear polarization results from ordered Si-O bonds. By taking into account an average interfacial width of 6 Å as determined by several techniques^{1,5} and an average terrace width of 15 Å (for monatomic steps when $\alpha=5^\circ$) we estimate that c_3 is generated in an area extending a distance of ~ 3 Å in the [011] direction either side of each step, i.e., ~ 2 Si-O bonds. This interpretation is supported by the TEM image of an interfacial monatomic step in Fig. 3(c) of Ref. 8 which shows the structure of an epitaxial oxide sublayer changing over approximately this distance. Macroscopically, the terrace interfacial structure is therefore either of a higher symmetry (C_{4v} or C_{6v}) or disordered yielding an isotropic response.²⁵

The C_{3v} symmetry at the steps and the macroscopically isotropic terrace oxide symmetry with respect to SHG impose strict limitations on the possible interfacial phases of c - SiO_2 . The growth mechanism of tridymite proposed by Ourmazd *et al.*⁵ places the c axis parallel to [011] and creates a macroscopic C_{4v} terrace c - SiO_2 symmetry resulting from a 90° rotation of the C_{2v} symmetry of each tridymite domain when a monatomic step is encountered. Our laser spot size is such that SHG originates from $\sim 30\,000$ terraces for the $\alpha=5^\circ$ monatomically stepped surface, and therefore SHG is sensitive to the macroscopic symmetry with a statistically high significance, in contrast to TEM.⁸ When tridymite grows across a monatomic step, a plane defect is created which can give rise to a C_{3v} symmetry axis normal to the interface by interrupting the hexagonal puckered ring structure.

After LTO, $|c_2|$ is much larger than the value from the NOS sample, while c_3 is similar in value. The increase in $|c_2|$ is in agreement with the tridymite model⁵ since the predominance of biatomic steps will give the tridymite a net C_{2v} symmetry, while the similar values of c_3 suggest

that the amount of tridymite present at the interface is almost invariant. Tridymite is therefore a good candidate for a possible epitaxial SiO_2 sublayer. However, it is important to note that Akatsu and Ohdomari⁹ were able to obtain similar TEM data to that obtained by Ourmazd *et al.* and co-workers^{3,5,8} in simulations of TEM images of rough interfaces with no intervening c - SiO_2 . Therefore, as acknowledged by Ourmazd *et al.*,⁵ the tridymite model is not unique to their TEM data. The same cautionary note must be applied to the above interpretation of the SHG data: it might be possible to construct other models which would give rise to qualitatively similar data. Therefore, at this juncture we can neither totally exclude nor completely corroborate the existence of an epitaxial oxide sublayer of the native grown SiO_2 . However, as discussed above, the large $|c_3|$ from both the NOS and LTO samples is strongly suggestive of the presence of crystalline order in the vicinity of the steps.

B. Sample after postoxidation annealing

In order to improve interfacial quality, such processing procedures as two-step oxidation and postoxidation annealing have been proposed.¹⁴ There is general agreement that annealing improves both electronic properties and interfacial flatness.¹⁵ In addition, information on the mechanisms underlying the interfacial stress and its influence on the SH response can be obtained from measurements made after various annealing treatments.¹¹ For this purpose several annealing cycles were performed on the Si(100): 5° NOS sample. In the first cycle the sample temperature was ramped from room temperature to 600°C at a rate of $10^\circ\text{C}/\text{min}$ and the sample was subsequently cooled to room temperature at the same rate. In the subsequent cycles the maximum temperature was increased successively by 50°C . Figure 4 shows the c_m coefficients of the SH rotational anisotropy as a function of the maximum annealing temperature taken at room temperature after each cycle.

The results presented in Fig. 4 show that within experi-

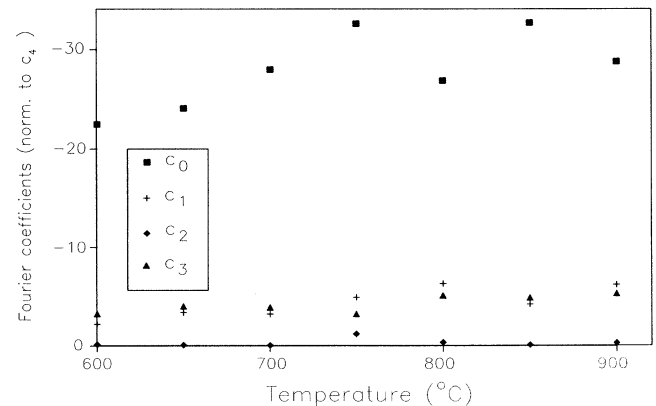


FIG. 4. The dependence of the SH Fourier coefficients obtained from NOS samples on postoxidation annealing as a function of the maximum annealing temperature. For details see text.

mental error the c_m remain constant after annealing except for the isotropic coefficient c_0 to which we return later. Govorkov *et al.*¹¹ found that the SH intensity from SiO₂/Si(111) samples, in which the oxide was highly stressed by a rapid cooling after oxidation, decreased by a factor of about 10 after an annealing cycle to 500 °C due to stress relaxation. On the other hand, samples that were oxidized in dry oxygen and cooled down gradually did not show any noticeable increase in the SH intensity or any change in its rotational dependence.¹¹ Therefore the existence of a large metastable stress-induced non-linearity can be considered unlikely because after post-oxidation annealing of the NOS samples the c_m coefficients of the SH response remain unchanged and are consistent with those obtained from the LTO samples. Note that this does not mean that there is no stress present at the buried interface, but merely that we do not observe a change in the amount of stress present as a result of postoxidation annealing. EerNisse established that large amounts of stress occurred in oxides grown at temperatures below 950 °C.¹⁶ More recently Fitch *et al.*¹⁷ have shown that there is always a substantial residual intrinsic interfacial stress on flat surfaces, which is independent of the growth temperature and thermal annealing. The surface step model proposed by Mott³¹ in conjunction with results of Leroy¹⁸ show how it may be possible to form SiO₂ on vicinal Si surfaces without the necessity for the buildup of a large intrinsic stress.¹⁹ If oxidation takes place predominantly at steps (edge or kink sites), the oxide film will advance with a volume expansion laterally as well as normal to the surface. In this manner a large fraction of stress will be relieved as the film grows.

After the first annealing cycle of the NOS sample, c_0 has changed sign and its magnitude has increased, but is similar to the value obtained from the LTO and the clean surface. Several models suggest that Si-Si dimers remain at the interface, whereas the hydrogen atoms in steam are known to eliminate interface states¹ and dimer states.¹³ In order to support the assertion that the change in the sign of c_0 is due to the presence of hydrogen at the interface, we have exposed the clean Si(100):5° surface to hydrogen until the SH response saturated. The c_m coefficients of the SH rotational dependence from the hydrogen saturated Si(100):5° surface are shown in Table I, and c_0 was found to be similar to the value obtained from the NOS sample. This observation can be explained in a spectroscopic manner. The photoemission spectra of Hansson and Uhrberg¹³ show that the surface dimer and dangling-bond states are located between 2 and 0.5 eV below the Fermi level, which is less than our SH photon energy (3.25 eV). On the other hand, these surface states are completely removed on the hydrogen-saturated Si(100) surface and two hydrogen-induced interfacial states occur at 4.8 and 5.6 eV below the Fermi level, which is greater than our SH photon energy. In both cases the SH response is nonresonant, but the phase of c_0 with respect to c_4 (where c_4 arises entirely from the bulk SH response) changes upon hydrogenation of the Si(100) surface. Therefore we suggest that Si dimers are still present at the interface after LTO but are not present on

the NOS samples. However the change in c_0 after annealing the NOS sample to 600 °C indicates the removal of hydrogen from the interface. This observation is supported by the secondary-ion mass-spectrometry studies of Johnson, Biegelsen, and Moyer,¹⁵ which show that the hydrogen concentration at the interface decreases significantly for annealing temperatures above 500 °C.

C. Thermal oxide samples

After HTO, the most striking result is a threefold increase in $|c_2|$ relative to LTO, which is contrary to the expectation that the monatomic steps present during HTO will eliminate the single domain character of the interface present after LTO. $|c_2|$ is the largest of the anisotropic coefficients, and it exceeds $|c_2|$ obtained from the clean surface.

The dominance of C_{2v} symmetry on this surface is incompatible with the model proposed by Ourmazd *et al.*,⁵ which leads to a macroscopic C_{4v} symmetry for a monatomically stepped surface. We point out that Fuoss *et al.*⁶ found that in the interfacial region order decays from the infinite long-range order of the Si(100) substrate through highly oriented microcrystallites embedded in an amorphous matrix and, finally, to a progressively sparser, more randomly oriented and more disordered microcrystalline-amorphous mixture. Experimental observations of similar oxide layers performed by Rochet *et al.*⁷ clearly show the presence of microcrystallites at the interface on a Si(100) substrate misoriented by 5° towards [011], a misorientation which is consistent with that of the substrate used in most of our experiments. Their experiments have shown that one can induce the formation of microcrystallites of *c*-SiO₂ after an oxidation treatment in dry O₂ at 800 °C. The presence of “long” (greater than 100 Å) [1 $\bar{1}$ 0] ledges along which epitaxy occurs allows the precise determination of the projected Si positions by TEM, so that they were able to propose models for this phase derived from the ideal β -cristobalite structure contracted along two crystal axes and elongated along the third.

The highly oriented, elongated microcrystallites of cristobalite induced by the presence of steps which have

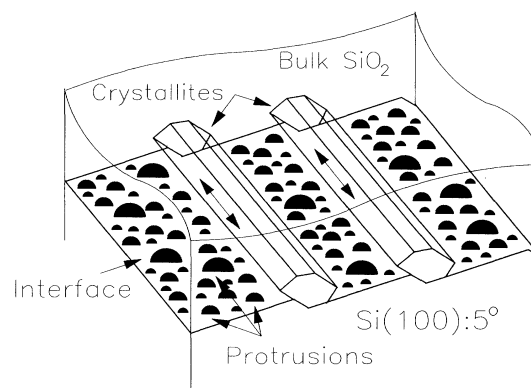


FIG. 5. Schematic representation of our model of the interface after HTO.

been observed by Rochet *et al.*⁷ are a very strong candidate for the microscopic origin of the large $|c_2|$ coefficient reported here. The contribution of faceting to $|c_2|$ would appear to be negligible because Rochet *et al.*⁴ have observed only (111) facets on such surfaces, and these ought to influence $|c_3|$ and not $|c_2|$. Figure 5 shows a sketch of our model of the SiO₂/Si(100):5° interface which has been grown at high temperature. Note the well-oriented microcrystallites which lead to a macroscopic twofold symmetry arising from the suggested structure by Rochet *et al.*⁷ of the nonideal β -cristobalite.

V. CONCLUSIONS

We have shown that the interfacial region on vicinal Si(100) surfaces covered with a native oxide possess macroscopic C_{1v} and C_{3v} symmetry. The magnitude of the SH intensity is consistent with the latter originating from a region of ~ 3 Å perpendicular to each step and is also consistent with the presence of a step-induced plane defect in an epitaxial c -SiO₂ layer of tridymite. The absence of C_{2v} symmetry from the native oxide interface grown in steam is consistent with the model proposed by Ourmazd *et al.* in which tridymite domains of C_{2v} symmetry are rotated by 90° at monatomic steps, leading to a macroscopic C_{4v} symmetry.⁵ In contrast to this, C_{2v} symmetry is clearly present after oxidation of the clean Si(100) surface in dry O₂ at different temperatures. For low temperatures, this is consistent with the presence of dimers at

the single domain buried interface, as well as being consistent with the resulting net C_{2v} symmetry of tridymite. However, neither of these interpretations applies to the interface present after high-temperature oxidation, in agreement with both Fuoss *et al.* and Rochet *et al.* who observed highly oriented microcrystallites of cristobalite after oxide growth at similar temperatures.^{6,7} Therefore, our data are consistent with the interpretation that the amount and structure of c -SiO₂ present at the interface is dependent on the oxidation temperature. SHG measurements of postoxidation annealing of the NOS samples are consistent with the amount of stress reduction occurring as a result of annealing being too small to be observed by SHG, and with hydrogen leaving the buried interface for a temperature below 600°C. SHG has been shown to be a powerful probe of the SiO₂/Si(100) interfacial structure since it can probe interfaces created by a wide variety of oxide growth conditions.

ACKNOWLEDGMENTS

We gratefully acknowledge the financial support of the Ontario Laser and Lightwave Research Centre, the Natural Science and Engineering Research Council of Canada and Alcan International Ltd. G.L. acknowledges support from the Deutsche Forschungsgemeinschaft. We thank S. Janz for helpful discussions on absolute SHG measurements, G. Rawlings for technical assistance, and C. Goh and G. Allan for a careful reading of the manuscript.

- ¹F. J. Himpsel, F. R. McFeely, A. Taleb-Ibrahimi, J. A. Yarmoff, and G. Hollinger, *Phys. Rev. B* **38**, 6084 (1988), and references therein.
- ²M. Niwano, H. Katakura, Y. Takeda, Y. Takakuwa, N. Miyamoto, A. Hiraiwa, and K. Yagi, *J. Vac. Sci. Technol. A* **9**, 195 (1991).
- ³A. Ourmazd, P. H. Fuoss, J. Bevk, and J. F. Morar, *Appl. Surf. Sci.* **41/42**, 365 (1989).
- ⁴F. Rochet, H. Roulet, G. Dufour, S. Carniato, G. Guillot, N. Barrett, and M. Froment, *Appl. Surf. Sci.* **59**, 117 (1992).
- ⁵A. Ourmazd, D. W. Taylor, J. A. Rentschler, and J. Bevk, *Phys. Rev. Lett.* **59**, 213 (1987).
- ⁶P. H. Fuoss, L. J. Norton, S. Brennan, and A. Fischer-Colbrie, *Phys. Rev. Lett.* **60**, 600 (1988).
- ⁷F. Rochet, M. Froment, C. D'Anterrosches, H. Roulet, and G. Dufour, *Philos. Mag. B* **59**, 339 (1989).
- ⁸A. Ourmazd, J. A. Rentschler, and J. Bevk, *Appl. Phys. Lett.* **53**, 743 (1988).
- ⁹H. Akatsu, and I. Ohdomari, *Appl. Surf. Sci.* **41/42**, 357 (1989).
- ¹⁰G. Renaud, P. H. Fuoss, A. Ourmazd, J. Bevk, B. S. Freer, and P. O. Hahn, *Appl. Phys. Lett.* **58**, 1044 (1991).
- ¹¹S. V. Govorkov, N. I. Koroteev, G. I. Petrov, I. L. Shumay, and V. V. Yakovlev, *Appl. Phys. A* **50**, 439 (1990).
- ¹²L. L. Kulyuk, D. A. Shutov, E. E. Strumban, and O. A. Aktsipetrov, *J. Opt. Soc. Am. B* **8**, 1766 (1991).
- ¹³G. V. Hansson and R. I. G. Uhrberg, *Surf. Sci. Rep.* **9**, 197 (1988).
- ¹⁴V. A. Yakovlev, Q. Liu, and E. A. Irene, *J. Vac. Sci. Technol. A* **10**, 427 (1992).
- ¹⁵N. M. Johnson, D. K. Biegelsen, and M. D. Moyer, *J. Vac. Sci. Technol.* **19**, 390 (1981).
- ¹⁶E. P. EerNisse, *Appl. Phys. Lett.* **35**, 8 (1979).
- ¹⁷J. T. Fitch, C. H. Bjorkman, G. Lucovsky, F. H. Pollak, and X. Yin, *J. Vac. Sci. Technol. A* **7**, 775 (1989).
- ¹⁸B. Leroy, *Philos. Mag. B* **55**, 159 (1987).
- ¹⁹E. Kobeda and E. A. Irene, *J. Vac. Sci. Technol. B* **5**, 15 (1987).
- ²⁰W. A. Tiller, *J. Electrochem. Soc.* **128**, 689 (1981).
- ²¹Y. R. Shen, *Nature (London)* **337**, 519 (1989).
- ²²G. L. Richmond, J. M. Robinson, and V. L. Shannon, *Prog. Surf. Sci.* **28**, 1 (1988).
- ²³R. W. J. Hollering, D. Dijkkamp, and H. B. Elswijk, *Surf. Sci.* **243**, 121 (1991).
- ²⁴C. W. van Hasselt, M. A. Verheijen, and Th. Rasing, *Phys. Rev. B* **42**, 9263 (1990).
- ²⁵J. E. Sipe, D. J. Moss, and H. M. van Driel, *Phys. Rev. B* **35**, 1129 (1987).
- ²⁶H. W. K. Tom, Ph.D. dissertation, UC Berkeley, 1984.
- ²⁷Misorientation from (100) permits bulk contributions to c'_1 , c'_2 , and c'_3 . For $\alpha=5^\circ$ their magnitudes are less than 0.5, 0.1, and 0.5, respectively. c_4 decreases by <1% in rotating from $\alpha=0^\circ$ to 5° , confirming that it can be considered constant.
- ²⁸O. L. Alerhand, A. N. Berker, J. D. Joannopoulos, D. Vanderbilt, R. J. Hamers, and J. E. Demuth, *Phys. Rev. Lett.* **64**, 2406 (1990).
- ²⁹For a surface with only C_{1v} symmetry, c_3 is expected to be nonzero because a contribution to $I_{s,p}^{(2\omega)}(\psi)$ varies as $\sin^2(\psi)\cos(\psi)$ which includes a term in $\cos(3\psi)$. See, e.g., G. Lüpke, G. Marowsky, R. Steinhoff, A. Friedrich, B. Pettinger, and D. M. Kolb, *Phys. Rev. B* **41**, 6913 (1990) for further discussion.
- ³⁰S. Janz, K. Pedersen, and H. M. van Driel, *Phys. Rev. B* **44**, 3943 (1991), and references therein.
- ³¹N. F. Mott, *Philos. Mag. A* **45**, 323 (1981).